Laboratory injection molder for the fabrication of polymeric porous poly-epsilon-caprolactone scaffolds for preliminary mesenchymal stem cells tissue engineering

Microelectronic Engineering 175 (2017) 12–16

Contents lists available at ScienceDirect

Microelectronic Engineering

journal homepage: www.elsevier.com/locate/mee

Research paper

Laboratory injection molder for the fabrication of polymeric porous poly-epsilon-caprolactone scaffolds for preliminary mesenchymal stem cells tissue engineering applications

Tania Limongi [a,*], Lucia Lizzul [b], Andrea Giugni [a], Luca Tirinato [a], Francesca Pagliari [c], Hua Tan [d], Gobind Das [a], Manola Moretti [e], Monica Marini [a], Giovanna Brusatin [b], Andrea Falqui [c], Bruno Torre [a], Cristiano di Benedetto [c], Enzo di Fabrizio [a]

[a] King Abdullah University of Science and Technology (KAUST), Physical Science and Engineering Division (PSE), SMILEs Laboratory, Thuwal 23955–6900, Saudi Arabia
[b] Department of Industrial Engineering, University of Padova, via Marzolo 9, 35131 Padova, Italy
[c] King Abdullah University of Science and Technology (KAUST), Biological and Environmental Sciences & Engineering Division (BESE), Bioscience program, Thuwal 23955–6900, Saudi Arabia
[d] King Abdullah University of Science and Technology (KAUST), Analytical Core Labs, Thuwal 23955–6900, Saudi Arabia
[e] King Abdullah University of Science and Technology (KAUST), Biological and Environmental Sciences & Engineering Division (BESE), Bioscience program and, Physical Science and Engineering Division (PSE), SMILEs Laboratory, Thuwal 23955–6900, Saudi Arabia

ARTICLE INFO

Article history:
Received 18 October 2016
Received in revised form 13 December 2016
Accepted 14 December 2016
Available online 16 December 2016

Keywords:
Biopolymers
Particulate leaching
Injection molding
Tissue engineering
Stem cells

ABSTRACT

This study presents a simple and rapid fabrication technique involving injection molding and particle leaching (IM/PL) to fabricate the porous scaffold for tissue engineering applications. Sodium Chloride (NaCl) and Sucrose are separately mixed with the poly-epsilon-caprolactone (PCL) granules using a screwed thermo-regulated extruder, then the biocompatible scaffolds are fabricated through injection molding. The micro/nano-structure of the samples and their different grade of porosity were characterized by scanning electron microscopy and mercury intrusion porosimetry. Bone marrow-derived mesenchymal stem cells are chosen for cell culture and Hoechst 33342 staining was used to verify the biocompatibility of the polymeric porous surfaces. We concluded that, by using the same fast solvent free injection/leaching process, the use of Sucrose as porogen, instead of NaCl, allowed the obtainment of biocompatible scaffolds with a higher grade of porosity with suitable cell adhesion capacity for tissue engineering purpose.

1. Introduction

Tissue engineering (TE) is a multidisciplinary science that by employing notions of materials science, engineering, medicine and biology try to develop functional biocompatible solutions to preserve, restore or improve cells, tissues and organs functionality [1]. The major issues in organ transplantation are the lack of donated organs and tissues as well as the immune rejection [2,3]. Although TE research in artificial organs implementation was greatly refined in the past decades, it still has to be optimized to improve all the related biocompatibility aspects. Biocompatible materials are a primary component of TE and regenerative medicine by providing structural and functional support to ensure the attachment, proliferation, and differentiation of specific cell populations. A variety of biomaterials has been extensively used for a wide range of in vitro and in vivo test [4–8] and significantly improved human health and quality of life. They can be commonly divided into three broad categories: metals, ceramics and polymers [9]. The last ones are extensively used as engineered scaffold material because of the possibility that scientists have to tune their physio-chemical characteristics such as surface features, porosity and degradability.

Natural polymers, chosen for the production of engineered scaffolds, are usually collagens, elastins, fibronectins and laminins compounds of the extracellular matrix (ECM) [10,11] that represent the non-cellular physical scaffolding material that provides and assists cells and tissues development and differentiation [12]. On the other hand, synthetic polymer has been optimized for tissue regeneration and regenerative medicine application and the most important advantages in their use lie in the possibility that scientists have to tune their mechanical physio-chemical characteristics such as surface features, porosity, and degradability. Polyesters include great number of biodegradable synthetic polymers like poly(glycolic acid) (PGA), poly(lactic acid) (PLA), poly(caprolactone) (PCL) and poly(propylene fumarate) (PPF). Their widespread use for medical application is due to the potential to degrade (the ester linkage is hydrolyzed) and to the possibility to tailor their degradation rate by changing their structure. The degradation products are, in some cases, resorbed through the metabolic pathways. PCL is a semicrystalline biocompatible and a non-toxic polyester

* Corresponding author.
E-mail address: tania.limongi@kaust.edu.sa (T. Limongi).

http://dx.doi.org/10.1016/j.mee.2016.12.014

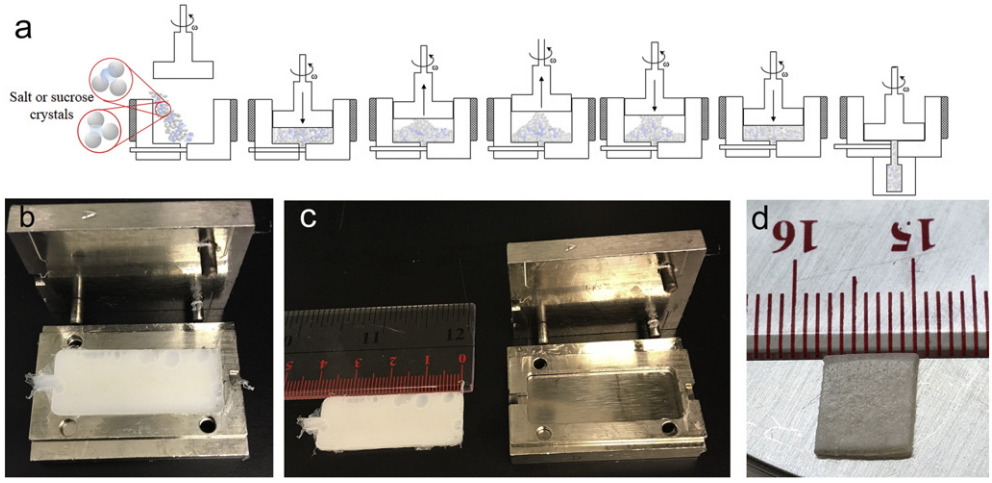

Fig. 1. a) Schematic representation depicts how the polymer and the porogens were mixed before the injection in the mold. Picture in b) shows the disassembled mold containing the just formed rectangular biocompatible surface that was recovered, c), and then cut in smaller square 0.7 cm side pieces d).

characterized by a low melting temperature and with a glass transition temperature of about −60 °C [13]. The preparation of PCL consists in the ring-opening polymerization of ε-caprolactone, the cyclic monomer. PCL degradation rate is lower compared to PLA and makes it useful for long-term medical implants; however, the speed of hydrolysis can be hastened by copolymerization [14].

Many fabrication techniques are available for the production of biocompatible porous scaffolds; the choice of the most appropriate one depends on the bulk and surface characteristics of the polymer and on the specific use to which the scaffold is intended. A suitable fabrication technique must have the possibility to confer to the engineered material the highest biocompatibility, and the correct grade of hydrophobicity/hydrophilicity and porosity to aid cell infiltration and to guarantee enough nutrient provision and waste products elimination. The production of porous 3D devices is mainly established on transforming biopolymers from the solid to the liquid phase, generally by dissolving or melting. These techniques comprise solvent and solvent-free casting/particle leaching (S and SF-CPL) [15–17], thermally-induced phase separation [18], gas foaming [19], electrospinning [20], 3D printing [21,22] and rapid prototyping [23].

The aim of this study was to fabricate porous PCL scaffolds by a solvent-free conventional injection molding and particle leaching (IM/PL) approach using two different porogens, NaCl and Sucrose. We characterized the micro- and nano-structure of the samples and measured their porosity and mechanical properties using scanning electron microscopy (SEM) and mercury intrusion porosimetry (MIP). Since stem cells (SCs) are commonly used cells in tissue engineering [24–26] application, bone marrow-derived mesenchymal stem cells were cultured on control flat bulk PCL surface and into the 2 different kinds of porous scaffolds and cell adhesion was tested by SEM imaging and Hoechst 33342 staining.

2. Materials and methods

2.1. Porous scaffold fabrication

The polymer employed to fabricate the scaffold was the PCL in pellets (Mn ~ 80,000, pellets, Sigma-Aldrich, 440744). To create the pores into the matrix, Sodium Chloride (NaCl, Sigma- Aldrich, S9888) and Sucrose (Sigma-Aldrich, 84097) crystals were utilized as porogens.

To reach the desired porogens dimension, both NaCl and Sucrose crystals were selected using cell dissociation sieves (CD-1 Sigma) with 70 and 380 μm Opening Size (O.S.). For the purpose, the crystals were roughly ground in a ceramic mortar with a pestle and then poured in the sieve with O.S. of 380 μm and sieved with the help of a glass pestle into a beaker. The crystals with a diameter minus of 380 μm were transferred in the sieve with O.S. of 70 μm. After sieving them, crystals with dimensions ranging from 70 to 380 μm were recovered from the sieve and stored ready to use. All the steps above described were performed under a chemical hood. To fabricate the scaffolds, the CSI-183IM laboratory injection molder was used; it allowed preparing a homogeneous mass of a melted polymer with one of each of the two different porogens. Using an adequate heat as well as proper mixing it is possible to inject the melt in a rectangular mold allowing the simultaneously realization of almost 10 porous biocompatible scaffolds of about 0.7 cm side (Fig. 1).

The microinjector mixer is head up till 150 °C and then used to mix PCL (Control), PCL and NaCl (NaCl scaffold) and PCL and Sucrose (Sucrose scaffold), each porogen was added to the polymer at the 30% (w/w). The process had duration of about 25 min considering the warm-up, mixing, pressing and the cooling down phases (Fig. 2).

Control, NaCl and Sucrose samples were fabricated setting a nominal 150 °C for both, mixing cup and mold. PCL pellets 3 g of porogen/PCL were used, and both Sodium Chloride and Sucrose were added in quantity of 30% wt/wt, resulting in 3 samples each subdivisible in 8 squared pieces, 7 mm sides.

The polymer/salt and polymer/Sucrose composites were then leached in hot (about 40 °C) Milli-Q water, with water changes every 12 h, for two weeks to remove all the porogens. The presence of NaCl content every 48 h was titrated by silver nitrate solution, until the sensitive silver nitrate test did not show any additional release of chloride ions into the water. The introduction of 5 drops of 0.1 M silver nitrate into 10 mL of rinse water, causes an immediately discoloration of it if the salt is present [27]. When no more precipitate was found, the sample was considered free of Sodium Chloride and the leaching process

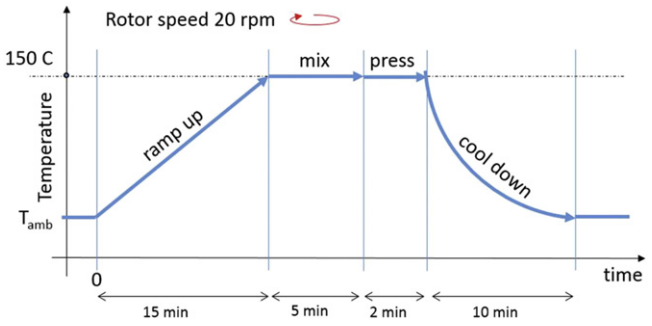

Fig. 2. Graphical view of the duration of the different phases of the scaffold fabrication process by referring to the different ranges of temperature.

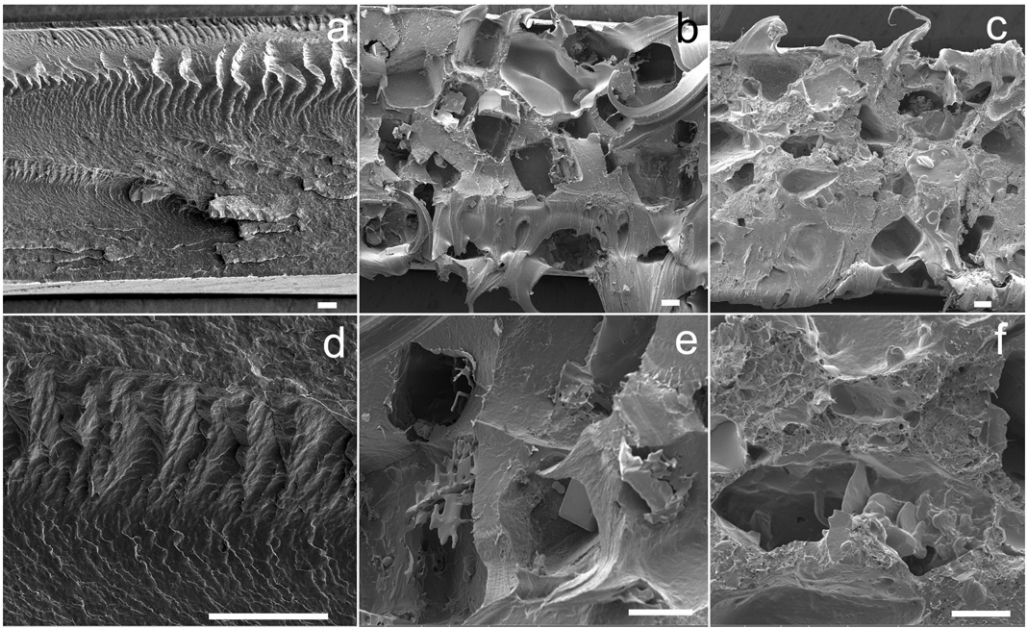

Fig. 3. Low and high magnification SEM images of PCL scaffold cross-sections: a) and d) refer to controls, b) and e) to Sodium Chloride use and c) and f) to Sucrose. Bars 100 μm.

completed. Sucrose residue in the scaffold was estimated every 48 h using Benedict's reduction test [28]. At the end of the leaching process scaffolds were dried in an oven at 40 °C for 24 h and stored in a desiccator.

2.2. Scaffold preparation and cell culture

Each PCL substrate was placed in a 12 well plate, sterilized by immersion in ethanol, washed twice in sterile water, dried in a laminar flow hood and further sterilized by UV irradiation for 2 h. Substrates were let float face down on complete medium basal medium (ATCC PCS-500-030) supplemented with 7% fetal bovine serum, 15 ng/mL recombinant human insulin-like growth factor-1 (rh IGF), 125 pg/mL recombinant human fibroblast growth factor beta (rh-FGF-b) and 2.4 mM L-Alanyl-L-Glutamine [growth kit (ATCC PCS-500-030)], 10 Units/mL Penicillin (Sigma Aldrich) and 10 μg/mL Streptomycin (Sigma Aldrich) for 7 days in a cell culture incubator (37 °C, 5% CO_2, 95% humidity). Before plating the cells, the medium was removed and substrates were washed and let dry in the biological cabinet for a couple of hours.

Bone marrow-derived mesenchymal stem cells (ATCC PCS-500-012) were cultured in the same medium described above we used to treat biocompatible surfaces. 40,000 cells were dropwise seeded on Control, NaCl and Sucrose scaffolds and after 40 min made up to volume with fresh medium. After 7 days, cells were fixed in PFA 2% for 15 min at room temperature (RT) and stained with Hoechst 33342 at 8 μM for 20 min. The experiment was performed in triplicate.

2.3. Confocal microscopy

Fluorescence images have been collected using a Zeiss LSM 710 upright confocal microscope with a Plan Apochromat 10× objective with a 0.45 numerical aperture. 4 different squares for each sample were taken and cells were counted using ImageJ cell counter plugin [27].

2.4. Scanning electron microscopy

To visualize the scaffold morphology and pore structure, the specimens were first freeze fractured in order to expose the cross section, immersed in liquid nitrogen and then broken using a couple of tweezers. In this way the scaffold architecture is not modified by plastic deformation allowing proper results. Surfaces were then sputtered with 10 nm of Gold using 20 mA as sputter current with a Cressington 208HR 8000 coater. SEM images were acquired through a Quanta 200 (FEI Company) scanning electron microscope operating at 5 kV with 10.5 mm as working distance.

2.5. Mercury intrusion porosimetry (MIP)

To determine pore size distribution and porosity, permeability and compressibility of the scaffolds the AutoPore IV (9500, Micromeritics, USA) mercury porosimeter was used. The samples were first evacuated to a pressure of 0.5 psia in order to remove physisorbed gasses from the interior of the sample. Porosimetry experiments were conducted with an equilibration time of 10 s, the pressure was increased incrementally

	Intrusion Data Summary			Pore Structure Summary	Material Compressibility	
	Total Intrusion Volume (mL/g)	*Average Pore Diameter (4V/A)*	*Porosity %*	*Permeability (mdarcy)*	*Linear Coefficient*	*Quadratic Coefficient*
Control	0.0535± 0.0014	0.0078 ± 0.0003	5.83 ± 0.14	0.06 ± 0.02	-2.74E-07	2.85E-13
PCL/NaCl	0.221±0.013	0.031 ± 0.002	17.5 ± 0.4	0.38 ± 0.14	-2.74E-07	2.85E-13
PCL/Sucrose	0.44±0.02	60 ± 3	34.7 ± 1.2	870 ± 110	-0.038059333	0.001288343

Fig. 4. MIP analysis results regarding intrusion, pore structure and material compressibility data. Average pore diameter is expressed in μm unit, V = volume; A = area.

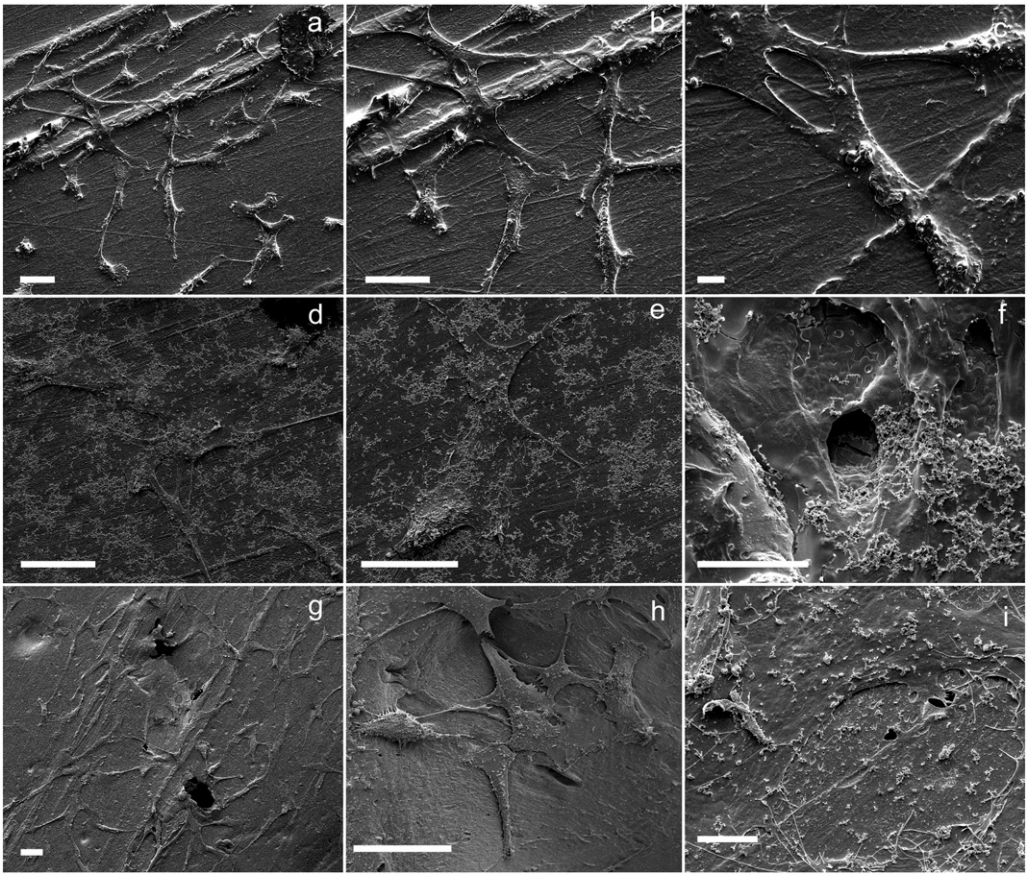

Fig. 5. SEM images of hMSC growth for 14 days on PCL control surface (a–c) and on PCL/NaCl (d–f), and PCL/Sucrose (g–i) porous scaffolds. Bars in a, b, d, e, g, h, are 50 μm and 10 μm in c, f, i.

from 0.5 psia to 60,000 psia, and then the pressure was decreased back to atmospheric pressure. For each sample, about 0.3 g of material was analyzed by using a 3 cm^3 penetrometer.

2.6. Statistical analysis

The data are presented as the mean ± Standard Error. Statistical analyses were performed using *t*-test for paired data; the difference was considered statistically significant at $p < 0.05$.

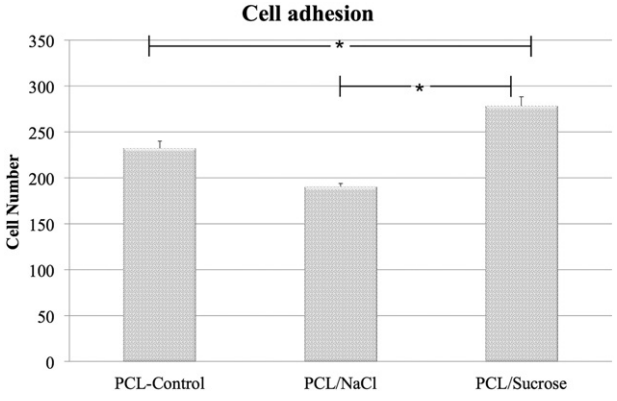

Fig. 6. Hoechst 33342 adhesion analysis done on day 14 of the culture; the bars indicate the number of adhered cells counted on the bulk PCL substrates and on the PCL/NaCl and PCL/Sucrose scaffolds.

3. Results

The presented injection/particulate leaching technique allowed the fabrication of 3 types of scaffolds. By imaging them with SEM resulted that PCL surface realized without porogens exhibited a well-defined compact structure (Fig. 3A and D) whereas, by using porogens, the substrates resulted characterized by well-distributed pore structures both for NaCl (Fig. 3B and E) and Sucrose (Fig. 3C and F). High-resolution SEM images allowed us to recognize some undissolved NaCl crystals (Fig. 5E) and the presence of smaller but numerous pores in the scaffold realized by using Sucrose (Fig. 5F). MIP analysis clearly showed (Fig. 4) as PCL/Sucrose sample, characterized by having a significantly ($p < 0.05$) higher total intrusion volume (0.44 mL/g) and higher average pore diameter (60 μm) resulted more porous (34.7%) than control (5.83%) and PCL/NaCl (17.5%) ones. Scaffold realized by using Sucrose instead of NaCl resulted also more permeable (870 versus 0.38 mDarcy) and compressible (-0.04 and 0.001 versus $-2.74 * 10^{-7}$ and $2.85 * 10^{-13}$ linear and quadratic regression coefficients) as showed in Fig. 4. Despite the fact that NaCl and Sucrose crystals had the same average diameter (70 ÷ 380 μm), the presented results evidenced that, after the leaching, Sucrose crystals assured a higher grade of porosity. It was related to the difference of the solubility of the 2 substances in water media, in fact, considering that the leaching of the crystals was done using water at 40 °C, in our process the solubility for NaCl and Sucrose was 36.37 and 235.6 g per 100 g of water respectively.

hMSCs were used for cellular characterization of the scaffolds, because of their friendly manipulability and differentiation prospective. SEM images showed that hMSCs, after 14 days of cell seeding, adhered, spread and grew on the surface of the PCL control (Fig. 5a–c), PCL/NaCl (Fig. 5d–f), and PCL/Sucrose (Fig. 5g–i), porous scaffolds. Some cells also adhered to the bulk PCL surface characterized by the presence of a certain grade of stochastic roughness (Fig. 5a–c). It was just discussed that

substrates with moderate roughness positively affect cell adhesion and growth [28–31]. Regarding in vitro test we performed with the porous surfaces, it has been shown that, the use of NaCl as porogen, during the IM/PL process, affected the attachment of the cells to the surface. In fact, it was evident since starting from the qualitative SEM analysis (Fig. 5d and e), that there were a less number of healthy cells and a higher saline residue (Fig. 5f) on the device fabricated using Sodium Chloride as porogen in respect to those realized without porogens or with Sucrose crystals. The largest number and the flat morphology of stem cells, well adherent, to the PCL/Sucrose substrate, put in evidence an appreciable spreading around (Fig. 5g) and in (Fig. 5h) the porous structure. Furthermore, the formation of numerous pseudopodia (Fig. 5h and i) indicated strong cellular adhesion and the scaffold after Sucrose leaching.

These outcomes were reinforced by simultaneous quantitative adhesion analysis done with nuclear stain Hoechst 33342 on days 14 of the culture. Adhesion of hMSCs grown on the 3 different kinds of scaffolds was compared as shown in Fig. 6. PCL/Sucrose scaffolds showed a higher number of cells growth on it with respect to PCL Control scaffolds (278 ± 10 versus 232 ± 8) and respect to PCL/NaCl ones (278 ± 10 versus 191 ± 4). These results suggested that porous scaffolds produced by leaching Sucrose assisted cell survival better than those obtained from PCL/NaCl mixture.

4. Conclusion

In this work we highlighted that the IM/PL method represents an optimal solution for the quick fabrication of porous biocompatible scaffold since it does not use the any kind of organic solvent and can be used also for mass production.

We verified that, by using the same fast solvent free injection/leaching process, the use of Sucrose as porogen, instead of NaCl, allowed the realization of biocompatible scaffolds with a higher grade of porosity also starting from crystals of the same diameter. The proposed solution supported a better adhesion and proliferation of mesenchymal stem cells. The higher solubility of Sucrose than that of Sodium Chloride assisted the production of scaffold with a functional grade of porosity and reduced the dissolution and recrystallization phenomena of the eventually un-leached porogens present in the inner zone of the porous surface when it is in the cellular media kept at 37 °C in the cell incubator. The biocompatibility and the tunable structural properties of the just presented scaffolds are strictly related to their future applications for a wide range of in vitro and in vivo tissue engineering tests.

References

[1] R. Langer, D.A. Tirrell, Designing materials for biology and medicine, Nature 428 (6982) (2004) 487–492.
[2] Xenotransplantation. Nat. Biotechnol. 18, IT53–IT55 (2000), http://dx.doi.org/10.1038/80100.
[3] M. Nasr, T. Sigdel, M. Sarwal, Advances in diagnostics for transplant rejection, Expert. Rev. Mol. Diagn. 16 (10) (2016) 1121–1132.
[4] E. Zanchetta, E. Guidi, G. Della Giustina, M. Sorgato, M. Krampera, G. Bassi, et al., Injection molded polymeric micropatterns for bone regeneration study, ACS Appl. Mater. Interfaces 7 (13) (2015) 7273–7281.
[5] P. Ferruti, N. Mauro, L. Falciola, V. Pifferi, C. Bartoli, M. Gazzarri, et al., Amphoteric, prevailingly cationic L-arginine polymers of poly(amidoamino acid) structure: synthesis, acid/base properties and preliminary cytocompatibility and cell-permeating characterizations, Macromol. Biosci. 14 (3) (2014) 390–400.
[6] V. Cauda, A. Chiodoni, M. Laurenti, G. Canavese, T. Tommasi, Ureteral double-J stents performances toward encrustation after long-term indwelling in a dynamic in vitro model, J. Biomed. Mater. Res. B Appl. Biomater. (2016) http://dx.doi.org/10.1002/jbm.b.33756.
[7] P. Wang, L. Zhao, J. Liu, M.D. Weir, X. Zhou, H.H.K. Xu, Bone tissue engineering via nanostructured calcium phosphate biomaterials and stem cells, Bone Res. 2 (2014) 14017.
[8] O.F. Khan, M.V. Sefton, Endothelialized biomaterials for tissue engineering applications in vivo, Trends Biotechnol. 29 (8) (2011) 379–387.
[9] M. Zhang, S.P. James, Biomaterials, Polymers. Encyclopedia of Medical Devices and Instrumentation, John Wiley & Sons, Inc., 2006
[10] Y. He, F. Lu, Development of synthetic and natural materials for tissue engineering applications using adipose stem cells, Stem Cells Int. 2016 (2016) 12.
[11] S.A. Sell, P.S. Wolfe, K. Garg, J.M. McCool, I.A. Rodriguez, G.L. Bowlin, The use of natural polymers in tissue engineering: a focus on electrospun extracellular matrix analogues, Polymer 2 (4) (2010) 522.
[12] C. Frantz, K.M. Stewart, V.M. Weaver, The extracellular matrix at a glance, J. Cell Sci. 123 (24) (2010) 4195–4200.
[13] P.A. Gunatillake, R. Adhikari, Biodegradable synthetic polymers for tissue engineering, Eur. Cell. Mater. 5 (2003) 1–16 (discussion).
[14] B.D. Ulery, L.S. Nair, C.T. Laurencin, Biomedical applications of biodegradable polymers, J. Polym. Sci. B Polym. Phys. 49 (12) (2011) 832–864.
[15] D. Sin, X. Miao, G. Liu, F. Wei, G. Chadwick, C. Yan, et al., Polyurethane (PU) scaffolds prepared by solvent casting/particulate leaching (SCPL) combined with centrifugation, Mater. Sci. Eng. C 30 (1) (2010) 78–85.
[16] L. Ma, W. Jiang, W. Li, Solvent-free fabrication of tissue engineering scaffolds with immiscible polymer blends, Int. J. Polym. Mater. 63 (10) (2014) 510–517.
[17] L. Tania, T. Luca, P. Francesca, G. Andrea, A. Marco, P. Gerardo, et al., Fabrication and applications of micro/nanostructured devices for tissue engineering, Nano-Micro Lett. 9 (1) (2017).
[18] R. Akbarzadeh, A.M. Yousefi, Effects of processing parameters in thermally induced phase separation technique on porous architecture of scaffolds for bone tissue engineering, J. Biomed. Mater. Res. B Appl. Biomater. 102 (6) (2014) 1304–1315.
[19] H. Yen-Chen, J.M. David, Gas foaming to fabricate polymer scaffolds in tissue engineering, Scaffolding in Tissue Engineering, CRC Press 2005, pp. 155–167.
[20] S.-J. Seo, H.-W. Kim, J.-H. Lee, Electrospun nanofibers applications in dentistry, J. Nanomater. 2016 (2016) 7.
[21] X. Li, R. Cui, L. Sun, K.E. Aifantis, Y. Fan, Q. Feng, et al., 3D-printed biopolymers for tissue engineering application, Int. J. Polym. Sci. 2014 (2014) 13.
[22] V. Baskaran, G. Štrkalj, M. Štrkalj, A. Di Ieva, Current applications and future perspectives of the use of 3D printing in anatomical training and neurosurgery, Front. Neuroanat. 10 (69) (2016).
[23] M.E. Hoque, Y.L. Chuan, I. Pashby, Extrusion based rapid prototyping technique: an advanced platform for tissue engineering scaffold fabrication, Biopolymers 97 (2) (2012) 83–93.
[24] T. Limongi, R. Schipani, A. Di Vito, A. Giugni, M. Francardi, B. Torre, et al., Photolithography and micromolding techniques for the realization of 3D polycaprolactone scaffolds for tissue engineering applications, Microelectron. Eng. 141 (2015) 135–139.
[25] N.C. Hunt, M. Lako, Tissue engineering using pluripotent stem cells: multidisciplinary approaches to accelerate bench-to-bedside transition, Regen. Med. 11 (6) (2016) 495–498.
[26] M. Sartori, S. Pagani, A. Ferrari, V. Costa, V. Carina, E. Figallo, et al., A new bi-layered scaffold for osteochondral tissue regeneration: in vitro and in vivo preclinical investigations, Mater. Sci. Eng. C 70 (2017) 101–111.
[27] C.A. Schneider, W.S. Rasband, K.W. Eliceiri, NIH Image to ImageJ: 25 years of image analysis, Nat. Methods 9 (7) (2012) 671–675.
[28] F. Gentile, L. Tirinato, E. Battista, F. Causa, C. Liberale, E.M. di Fabrizio, et al., Cells preferentially grow on rough substrates, Biomaterials 31 (28) (2010) 7205–7212.
[29] T. Limongi, F. Cesca, F. Gentile, R. Marotta, R. Ruffilli, A. Barberis, et al., Nanostructured superhydrophobic substrates trigger the development of 3D neuronal networks, Small 9 (3) (2013) 402–412.
[30] F. Cesca, T. Limongi, A. Accardo, A. Rocchi, M. Orlando, V. Shalabaeva, et al., Fabrication of biocompatible free-standing nanopatterned films for primary neuronal cultures, RSC Adv. 4 (86) (2014) 45696–45702.
[31] F. Gentile, R. La Rocca, G. Marinaro, A. Nicastri, A. Toma, F. Paonessa, et al., Differential cell adhesion on mesoporous silicon substrates, ACS Appl. Mater. Interfaces 4 (6) (2012) 2903–2911.